

Riccardo Bardin, Fleurianne Bertrand, Olena Palii, and Matthias Schlottbom

# A phase-space discontinuous Galerkin scheme for the radiative transfer equation in slab geometry

**Abstract:** We derive and analyze a symmetric interior penalty discontinuous Galerkin scheme for the approximation of the second-order form of the radiative transfer equation in slab geometry. Using appropriate trace lemmas, the analysis can be carried out as for more standard elliptic problems. Supporting examples show the accuracy and stability of the method also numerically, for different polynomial degrees. For discretization, we employ quad-tree grids, which allow for local refinement in phase-space, and we show exemplarily that adaptive methods can efficiently approximate discontinuous solutions. We investigate the behavior of hierarchical error estimators and error estimators based on local averaging.

**Keywords:** radiative transfer, discontinuous Galerkin, slab geometry, phase-space

## 1 Introduction

We consider the numerical solution of the radiative transfer equation in slab geometry, which has several applications such as atmospheric science [22], oceanography [4], pharmaceutical powders [7] or solid state lightning [30]; see also [8] for a recent introduction. In view of available well-posedness results [2], it is natural to assume that the total cross section  $\sigma_t$ , which is the sum of the scattering cross section  $\sigma_s$  and the absorption cross section  $\sigma_a$ , is strictly positive. In this situation, the radiative transfer equation is equivalent to the following second-order form of radiative transfer equation with Robin boundary conditions [14, 31],

$$-\partial_z \left( \frac{\mu^2}{\sigma_t} \partial_z u \right) + \sigma_t u = \sigma_s \int_0^1 u(\cdot, \mu') d\mu' + f \quad \text{in } \Omega, \quad (1)$$

$$u + \frac{\mu}{\sigma_t} \partial_n u = g \quad \text{on } \Gamma. \quad (2)$$

Here,  $u(z, \mu)$  corresponds to the even part of the solution of the radiative transfer equation for  $(z, \mu) \in \Omega = (0, L) \times (0, 1)$ . Furthermore,  $\partial_n u(0, \mu) = -\partial_z u(0, \mu)$  and  $\partial_n u(L, \mu) = \partial_z u(L, \mu)$  are the normal derivatives of  $u$  on the boundary of the slab, defined as  $\Gamma = \Gamma_0 \cup \Gamma_L$ , where  $\Gamma_z = \{z\} \times (0, 1)$ . The functions  $f$  and  $g$  model volume and boundary sources, respectively.

Due to the product structure of  $\Omega$ , it seems natural to use separate discretization techniques for the spatial variable  $z$  and the angular variable  $\mu$ . This is for instance done in the spherical harmonics method, in which a truncated Legendre polynomial expansion is employed to discretize  $\mu$  [13]. The resulting coupled system of Legendre moments, which still depend on  $z$ , is then discretized for instance by finite differences or finite elements [13]. Another class of approximations consists of discrete ordinates methods which perform a collocation in  $\mu$  and the integral in eq. (1) is approximated by a quadrature rule [13]. The resulting system of transport equations is then discretized for instance by finite differences [13] or discontinuous Galerkin methods [21, 19], and also spatially adaptive schemes have been used [33].

A major drawback of the independent discretization of the two variables  $z$  and  $\mu$  is that a local refinement in phase-space is not possible. Such local refinement is generally necessary to achieve optimal schemes. For instance, in slab geometry, the solution can be non-smooth in the two points  $(z, \mu) = (0, 0)$

and  $(z, \mu) = (L, 0)$ , which are exactly the two points separating the inflow from the outflow boundary. Although certain tensor-product grids can resolve this geometric singularity for the slab geometry, such as double Legendre expansions [13], they fail to do so for generic multi-dimensional situations. Moreover, local singularities of the solution due to the optical parameters or the source terms can in general not be resolved with optimal complexity.

Phase-space discretizations have been used successfully for radiative transfer in several applications, see, e.g., [10, 27, 28, 29] for slab geometry, [25] for geometries with spherical symmetries, or [15, 26] for more general geometries. Let us also refer to [24] for a phase-space discontinuous Galerkin method for the nonlinear Boltzmann equation. A non-tensor product discretization that combines ideas of discrete ordinates to discretize the angular variable with a discontinuous Petrov-Galerkin method to discretize the spatial variable has been developed in [9].

In this work, we aim to develop a numerical method for (1)–(2) that allows for local mesh refinement in phase-space and that allows for a relatively simple analysis and implementation. To accomplish this, we base our discretization on a partition of  $\Omega$  such that each element in that partition is the Cartesian product of two intervals. Local approximations are then constructed from products of polynomials defined on the respective intervals. Since such partitions generically contain hanging nodes, global approximations are generally discontinuous. Therefore, we employ a symmetric interior penalty discontinuous Galerkin formulation. Besides the proper treatment of traces, which requires the inclusion of a weight function in our case, the analysis of the overall scheme is along the standard steps for the analysis of discontinuous Galerkin methods [11]. As a result, we obtain a scheme that enjoys an abstract quasi-best approximation property in a mesh-dependent energy norm. Our choice of meshes also allows to explicitly estimate the constants in auxiliary tools, such as inverse estimates and discrete trace inequalities. As a result, we can give an explicit lower bound on the penalty parameter required for discrete stability. Our theoretical results about accuracy and stability of the method are confirmed by numerical examples, which show optimal convergence rates for different polynomial degrees assuming sufficient regularity of the solution. Moreover, we show that adaptively refined grids are able to efficiently construct approximations to non-smooth solutions.

For the local adaptation of the grid we investigate several error estimators. First, we consider two hierarchical error estimators, which use polynomials of higher degree, and the discrete solution on a uniformly refined mesh, respectively. Such estimators have been investigated in the elliptic context, e.g., in [5, 23]. Our numerical results show that these error indicators can be used to refine the mesh towards the singularity of the solution. A drawback of these estimators is that an additional global problem has to be solved in every step. Since the solutions to (1)–(2) can be discontinuous in  $\mu$ , the proofs developed for elliptic equations to show that the global estimator is equivalent to a locally computable quantity, see, e.g., [23], do not apply. To overcome the computational complexity of building estimators that require to solve a global problem, we propose an *a posteriori* estimator based on a local averaging procedure. This cheap estimator shows a similar performance compared to the more expensive hierarchical ones mentioned before.

The outline of the rest of the manuscript is as follows. In Section 2 we introduce notation and collect technical tools, such as trace theorems. In Section 3 we derive and analyze the discontinuous Galerkin scheme. Section 4 presents numerical examples confirming the theoretical results of Section 3. Section 5 shows that our scheme works well with adaptively refined grids. We introduce here two hierarchical error estimators and one based on local post-processing. The paper closes with some conclusions in Section 6.

## 2 Preliminaries

We denote by  $L^2(\Omega)$  the usual Hilbert space of square integrable functions and denote the corresponding inner product by

$$(u, v) = \int_{\Omega} u(z, \mu)v(z, \mu) d(z, \mu).$$

Furthermore, we introduce the Hilbert space

$$V = \{v \in L^2(\Omega) : \mu \partial_z v \in L^2(\Omega)\},$$

which consists of square integrable functions for which the weighted derivative is also square integrable; see [2, Section 2.2]. We endow the space  $V$  with the graph norm

$$\|v\|_V^2 = \|v\|_{L^2(\Omega)}^2 + \|\mu \partial_z v\|_{L^2(\Omega)}^2, \quad v \in V.$$

To treat the boundary condition eq. (2), let us introduce the following inner product

$$\langle u, v \rangle = \int_{\Gamma} uv \mu d\mu = \int_0^1 (u(L, \mu)v(L, \mu) + u(0, \mu)v(0, \mu)) \mu d\mu,$$

and the corresponding space  $L^2(\Gamma; \mu)$  of all measurable functions  $v$  such that

$$\|v\|_{L^2(\Gamma; \mu)}^2 = \langle v, v \rangle < \infty.$$

According to [2, Theorem 2.8], functions in  $V$  have a trace on  $\Gamma$  and

$$\|v\|_{L^2(\Gamma; \mu)} \leq \frac{2}{\sqrt{1 - \exp(-L)}} \|v\|_V. \quad (3)$$

For the analysis of the numerical scheme, we provide a slightly different trace lemma.

**Lemma 1.** Let  $K = (z^l, z^r) \times (\mu^b, \mu^t) \subset \Omega$  for  $0 \leq z^l < z^r \leq L$  and  $0 \leq \mu^b < \mu^t \leq 1$ . Let  $F = \{z_F\} \times (\mu^b, \mu^t)$  with  $z_F \in \{z^l, z^r\}$  be a vertical face of  $K$ . Then, for every  $v \in V$  it holds that

$$\int_F |v|^2 \mu d\mu \leq \left( \frac{\mu^t}{z^r - z^l} \|v\|_{L^2(K)} + 2\|\mu \partial_z v\|_{L^2(K)} \right) \|v\|_{L^2(K)}.$$

*Proof.* Without loss of generality, we assume that  $z^l = z_F = 0$  and  $z^r = h_z$ . From the fundamental theorem of calculus, we obtain that

$$w(0, \mu) = w(z, \mu) - \int_0^z \partial_z w(y, \mu) dy.$$

Multiplication by  $\mu$  and integration over  $K$  yields the inequality

$$h_z \int_F |w| \mu d\mu \leq \int_K |w| \mu d(z, \mu) + \int_K \int_0^z \mu |\partial_z w(y, \mu)| dy d(z, \mu).$$

Setting  $w = v^2$  in the previous inequality, observing that  $|\mu \partial_z w| \leq 2|(\mu \partial_z v)v|$  and applying the Cauchy-Schwarz inequality shows that

$$\int_F |v|^2 \mu d\mu \leq \int_K |v|^2 \frac{\mu}{h_z} d(z, \mu) + 2\|\mu \partial_z v\|_{L^2(K)} \|v\|_{L^2(K)},$$

which concludes the proof. □

## 2.1 Weak formulation and solvability

Performing the usual integration-by-parts, see also [31], the weak formulation of (1)–(2) is as follows.

Find  $u \in V$  such that

$$a^e(u, v) = (f, v) + \langle g, v \rangle \quad \forall v \in V, \quad (4)$$

with bilinear form  $a^e : V \times V \rightarrow \mathbb{R}$ ,

$$a^e(u, v) = \left( \frac{1}{\sigma_t} \mu \partial_z u, \mu \partial_z v \right) + (\sigma_t u, v) - (\sigma_s P u, v) + \langle u, v \rangle. \quad (5)$$

Here, for ease of notation, we use the scattering operator  $P : L^2(\Omega) \rightarrow L^2(\Omega)$ ,

$$(Pu)(z, \mu) = \int_0^1 u(z, \mu') d\mu'.$$

Under the assumptions  $0 \leq \sigma_s, \sigma_t \in L^\infty(0, L)$ ,  $\sigma_t - \sigma_s \geq c > 0$ ,  $f \in L^2(\Omega)$  and  $g \in L^2(\Gamma; \mu)$ , the weak solution  $u \in V$  of eq. (4) exists by the Lax-Milgram lemma, cf., e.g., [11, Lemma 1.4]. For  $\mu > 0$  fixed, problem (1)-(2) reduces to an elliptic problem for  $u(\cdot, \mu)$  and smoothness of  $z \mapsto u(z, \mu)$  is governed by the smoothness of the data and the coefficients [18]. Therefore, since  $f \in L^2(\Omega)$ , we have that the flux  $\frac{\mu}{\sigma_t} \partial_z u \in V$ . In particular, for a.e. fixed  $\mu > 0$ , the flux  $\frac{\mu}{\sigma_t} \partial_z u$  is continuous as a function of  $z \in (0, L)$ . We denote the space of regular solutions  $u$  by

$$V_* = \left\{ u \in V : \frac{\mu}{\sigma_t} \partial_z u \in V \right\}. \quad (6)$$

### 3 Discontinuous Galerkin scheme

In the following we will derive the numerical scheme to approximate solutions to eq. (4). After introducing a suitable partition of  $\Omega$  using quad-tree grids and corresponding broken polynomial spaces, we can essentially follow the standard procedure for elliptic problems, cf. [11]. One notable difference is that we need to incorporate the weight function  $\mu$  on the faces.

#### 3.1 Mesh and broken polynomial spaces

Discontinuous Galerkin methods can be formulated for rather general meshes. In order to simplify the presentation, and subsequently the implementation, we consider quad-tree meshes [17] as follows. Let  $\mathcal{T}$  be a partition of  $\Omega$  such that

$$K = (z_K^l, z_K^r) \times (\mu_K^l, \mu_K^r) \quad \forall K \in \mathcal{T},$$

for illustration see Figure 1. We denote the local mesh size by  $h_K = z_K^r - z_K^l$ .

Next, let us introduce some standard notation. Denote  $\mathbb{P}_k$  the space of polynomials of one real variable of degree  $k \geq 0$ , and let the broken polynomial space  $V_h$  be denoted by

$$V_h = \{v \in L^2(\Omega) : v|_K \in \mathbb{P}_{k+1} \otimes \mathbb{P}_k \quad \forall K \in \mathcal{T}\}. \quad (7)$$

Moreover, let  $V(h) = V + V_h$ . By  $\mathcal{F}_h^{vi}$  we denote the set of interior vertical faces, that is for any  $F \in \mathcal{F}_h^{vi}$  there exist two disjoint elements

$$K_1 = (z_1^l, z_1^r) \times (\mu_1^l, \mu_1^r) \text{ and } K_2 = (z_2^l, z_2^r) \times (\mu_2^l, \mu_2^r)$$

such that  $z_F = z_2^r = z_1^l$  and  $F = \{z_F\} \times ((\mu_1^l, \mu_1^r) \cap (\mu_2^l, \mu_2^r))$ . For  $F \in \mathcal{F}_h^{vi}$  we define the jump and the average of  $v \in V_h$  by

$$\llbracket v \rrbracket = v|_{K_1}(z_F, \mu) - v|_{K_2}(z_F, \mu), \quad \{v\} = \frac{1}{2}(v|_{K_1}(z_F, \mu) + v|_{K_2}(z_F, \mu)).$$

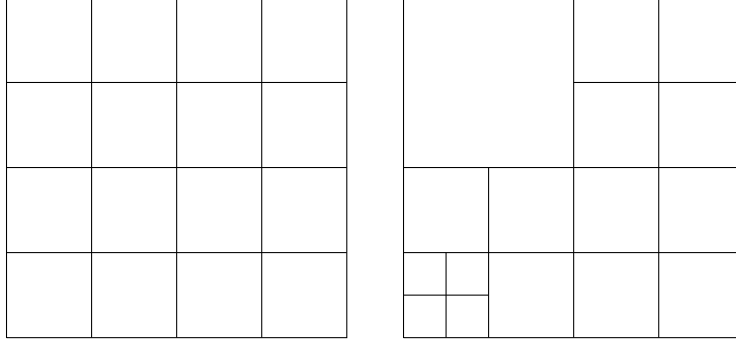


**Fig. 1:** Left: Uniform mesh with 16 elements. Right: Non-uniform mesh with hanging nodes.

Using the local mesh size  $h_{K_i}$ ,  $i \in \{1, 2\}$ , of the element  $K_i$  in  $z$ -direction, we define the averaged mesh-size  $H_F = (1/h_{K_1} + 1/h_{K_2})^{-1}$ , which should not be confused with the length of the face  $F$ . For an interior face  $F \in \mathcal{F}_h^{vi}$  with  $F = \{z_F\} \times (\mu_F^b, \mu_F^t)$ , which is shared by two elements  $K_F^i \in \mathcal{T}$ ,  $i = 1, 2$ , as above, let us introduce the sub-elements

$$E_F^i = (z_i^l, z_i^r) \times (\mu_F^b, \mu_F^t) \subset K_F^i. \quad (8)$$

We note that the inclusion in eq. (8) can be strict in the case of hanging nodes, see for instance Figure 1.

Combining Lemma 1 with common inverse inequalities, cf. [6, Sect. 4.5], i.e., for any  $k \geq 0$  there exists a constant  $C_{ie}(k)$  such that

$$\left( \int_{z^l}^{z^r} |v'|^2 dz \right)^{1/2} \leq \frac{\sqrt{C_{ie}}}{z^r - z^l} \left( \int_{z^l}^{z^r} |v|^2 dz \right)^{1/2} \quad \forall v \in \mathbb{P}_k, \quad (9)$$

we obtain the following discrete trace lemma.

**Lemma 2** (Discrete trace inequality). Let  $K = (z_K^l, z_K^r) \times (\mu_K^l, \mu_K^r) \in \mathcal{T}$  and let  $F = \{z_F\} \times (\mu_F^b, \mu_F^t) \in \mathcal{F}_h^v$  be such that  $F \subset \partial K$ . Then, for any  $k \geq 0$  there holds

$$\|v\|_{L^2(F; \mu)}^2 \leq \frac{C_{dt}}{h_K} \|v\|_{L^2((z_K^l, z_K^r) \times (\mu_F^b, \mu_F^t))}^2 \quad \forall v \in \mathbb{P}_k,$$

where  $C_{dt}(k) = 1 + \sqrt{C_{ie}(k)}$ , and  $C_{ie}$  is the constant in eq. (9).

### 3.2 Derivation of the DG scheme

In order to extend the bilinear form defined in eq. (5) to the broken space  $V_h$ , we denote with  $\partial_z^h$  the broken derivative operator such that

$$\left( \frac{\mu^2}{\sigma_t} \partial_z^h u_h, \partial_z^h v_h \right) = \sum_{K \in \mathcal{T}} \int_K \frac{\mu^2}{\sigma_t} \partial_z u_h \partial_z v_h d(z, \mu)$$

for  $u_h, v_h \in V_h$ . In view of eq. (4), let us then introduce the bilinear form

$$a_h^e(u, v) = \left( \frac{\mu^2}{\sigma_t} \partial_z^h u, \partial_z^h v \right) + (\sigma_t u, v) - (\sigma_s P u, v) + \langle u, v \rangle,$$

which is defined on  $V(h)$ . Note that  $a^e$  and  $a_h^e$  coincide on  $V$ . A routine calculation, cf. [11, Chapter 4], yields for any solution  $u \in V_*$  to (1)–(2) and  $v \in V_h$  that

$$a_h^e(u, v) = (f, v) + \langle g, v \rangle + \sum_{F \in \mathcal{F}_h^{vi}} \int_F \left( \left\{ \left\{ \frac{\mu}{\sigma_t} \partial_z^h u \right\} \right\} [v] + \left[ \left[ \frac{\mu}{\sigma_t} \partial_z^h u \right] \right] \{v\} \right) \mu d\mu.$$

Since  $\left[\left[\frac{\mu}{\sigma_t} \partial_z^h u\right]\right] = 0$  for all  $F \in \mathcal{F}_h^{v_i}$  by  $z$ -continuity of the flux of  $u \in V_*$ , we arrive at the identity

$$a_h^e(u, v) = (f, v) + \langle g, v \rangle + \sum_{F \in \mathcal{F}_h^{v_i}} \int_F \left\{ \left\{ \frac{\mu}{\sigma_t} \partial_z^h u \right\} \right\} \llbracket v \rrbracket \mu d\mu.$$

Hence, a consistent bilinear form is given by

$$a_h^c(u, v) = a_h^e(u, v) - \sum_{F \in \mathcal{F}_h^{v_i}} \int_F \left\{ \left\{ \frac{\mu}{\sigma_t} \partial_z^h u \right\} \right\} \llbracket v \rrbracket \mu d\mu,$$

which, for  $V_{*h} = V_* + V_h$ , is well-defined on  $V_{*h} \times V_h$ . Using that  $\llbracket u \rrbracket = 0$  for any  $u \in V$ , we arrive at the following symmetric and consistent bilinear form

$$a_h^{cs}(u, v) = a_h^e(u, v) - \sum_{F \in \mathcal{F}_h^{v_i}} \int_F \left( \left\{ \left\{ \frac{\mu}{\sigma_t} \partial_z^h u \right\} \right\} \llbracket v \rrbracket + \left\{ \left\{ \frac{\mu}{\sigma_t} \partial_z^h v \right\} \right\} \llbracket u \rrbracket \right) \mu d\mu,$$

which is again well-defined on  $V_{*h} \times V_h$ . We note that the summation over the vertical faces on the boundary  $\Gamma$  is included in the term  $\langle u, v \rangle$  in  $a_h^e$ . The stabilized bilinear form is then defined on  $V_{*h} \times V_h$  by

$$a_h(u, v) = a_h^{cs}(u, v) + \sum_{F \in \mathcal{F}_h^{v_i}} \frac{\alpha_F}{H_F} \int_F \llbracket u \rrbracket \llbracket v \rrbracket \mu d\mu, \quad (10)$$

with positive penalty parameter  $\alpha_F > 0$ , which will be specified below. Since  $\llbracket u \rrbracket = 0$  on any  $F \in \mathcal{F}_h^{v_i}$  and  $u \in V$ , it follows that  $a_h$  is consistent, i.e., for  $u \in V_*$  it holds

$$a_h(u, v_h) = a^e(u, v_h) \quad \forall v_h \in V_h. \quad (11)$$

The discrete variational problem is formulated as follows: Find  $u_h \in V_h$  such that

$$a_h(u_h, v_h) = (f, v_h) + \langle g, v_h \rangle \quad \forall v_h \in V_h. \quad (12)$$

### 3.3 Analysis

For the analysis of (12), let us introduce mesh-dependent norms

$$\|v\|_{V_h}^2 = a_h^e(v, v) + \sum_{F \in \mathcal{F}_h^{v_i}} H_F^{-1} \|\llbracket v \rrbracket\|_{L^2(F; \mu)}^2, \quad v \in V(h), \quad (13a)$$

$$\|v\|_*^2 = \|v\|_{V_h}^2 + \sum_{F \in \mathcal{F}_h^{v_i}} \frac{H_F}{C_{dt}} \left\| \left\{ \left\{ \frac{\mu}{\sigma_t} \partial_z^h v \right\} \right\} \right\|_{L^2(F; \mu)}^2, \quad v \in V_{*h}. \quad (13b)$$

In order to show discrete stability and boundedness of  $a_h$ , we will use the following auxiliary lemma.

**Lemma 3** (Auxiliary lemma). Let  $F \in \mathcal{F}_h^{v_i}$  be shared by the elements  $K_F^1, K_F^2 \in \mathcal{T}$ . Then, for  $w \in V_h$  and  $v \in V(h)$  it holds that

$$\int_F \left\{ \left\{ \frac{\mu}{\sigma_t} \partial_z^h w \right\} \right\} \llbracket v \rrbracket \mu d\mu \leq \frac{\sqrt{C_{dt}}}{2\sqrt{H_F}} \left( \sum_{i=1,2} \left\| \left\{ \left\{ \frac{\mu}{\sigma_t} \partial_z^h w \right\} \right\} \right\|_{L^2(E_F^i)}^2 \right)^{1/2} \|\llbracket v \rrbracket\|_{L^2(F; \mu)},$$

with  $C_{dt} = C_{dt}(k)$  from Lemma 2 and sub-elements  $E_F^i$ ,  $i = 1, 2$ , defined in eq. (8).

*Proof.* By definition of the average, we have that

$$\int_F \left\{ \left\{ \frac{\mu}{\sigma_t} \partial_z^h w \right\} \right\} \llbracket v \rrbracket \mu d\mu = \frac{1}{2} \int_F \frac{\mu}{\sigma_t} \partial_z w_1 \llbracket v \rrbracket \mu d\mu + \frac{1}{2} \int_F \frac{\mu}{\sigma_t} \partial_z w_2 \llbracket v \rrbracket \mu d\mu,$$

where  $w_1, w_2$  denote the restrictions of  $w$  to  $K_F^1$  and  $K_F^2$ , respectively. To estimate the first integral on the right-hand side, we employ the Cauchy-Schwarz inequality to obtain

$$\int_F \frac{\mu}{\sigma_t} \partial_z w_1 \llbracket v \rrbracket \mu d\mu \leq \left\| \frac{\mu}{\sigma_t} \partial_z w_1 \right\|_{L^2(F; \mu)} \|\llbracket v \rrbracket\|_{L^2(F; \mu)} \leq \frac{\sqrt{C_{dt}(k)}}{\sqrt{h_{K_F^1}}} \left\| \frac{\mu}{\sigma_t} \partial_z w_1 \right\|_{L^2(E_F^1)} \|\llbracket v \rrbracket\|_{L^2(F; \mu)},$$

where we used in the second step Lemma 2 applied to  $\frac{\mu}{\sigma_t} \partial_z w_1$ , which is a piecewise polynomial of degree  $k$ . A similar estimate holds for the second integral. Hence, we can estimate

$$\int_F \left\{ \left\{ \frac{\mu}{\sigma_t} \partial_z w \right\} \llbracket v \rrbracket \right\} \mu d\mu \leq \frac{\sqrt{C_{dt}}}{2} \left( \left\| \frac{\mu}{\sigma_t} \partial_z w \right\|_{L^2(E_F^1)}^2 + \left\| \frac{\mu}{\sigma_t} \partial_z w \right\|_{L^2(E_F^2)}^2 \right)^{1/2} \sqrt{\frac{1}{h_{K_F^1}} + \frac{1}{h_{K_F^2}}} \|\llbracket v \rrbracket\|_{L^2(F; \mu)},$$

which concludes the proof.  $\square$

The auxiliary lemma allows to bound the consistency terms in  $a_h$ , which gives discrete stability of  $a_h$ .

**Lemma 4** (Discrete stability). For any  $v \in V_h$  it holds that

$$a_h(v, v) \geq \frac{1}{2} \|v\|_{V_h}^2$$

provided that  $\alpha_F \geq 1/2 + C_{dt}(k)$  with constant  $C_{dt}(k)$  given in Lemma 2.

*Proof.* Let  $v_h \in V_h$ , and consider

$$a_h(v_h, v_h) = a_h^e(v_h, v_h) - 2 \sum_{F \in \mathcal{F}_h^{v_i}} \int_F \left\{ \left\{ \frac{\mu}{\sigma_t} \partial_z v_h \right\} \llbracket v_h \rrbracket \right\} \mu d\mu + \sum_{F \in \mathcal{F}_h^{v_i}} \frac{\alpha_F}{H_F} \int_F \llbracket v_h \rrbracket^2 \mu d\mu.$$

Using Lemma 3, and the fact that each sub-element  $E_F^i$  touches at most two interior faces, an application of the Cauchy-Schwarz yields for any  $\epsilon > 0$ ,

$$2 \sum_{F \in \mathcal{F}_h^{v_i}} \int_F \left\{ \left\{ \frac{\mu}{\sigma_t} \partial_z v_h \right\} \llbracket v_h \rrbracket \right\} \mu d\mu \leq \epsilon \left\| \frac{\mu}{\sigma_t} \partial_z^h v_h \right\|_{L^2(\Omega)}^2 + \sum_{F \in \mathcal{F}_h^{v_i}} \frac{C_{dt}}{2\epsilon H_F} \int_F \llbracket v_h \rrbracket^2 \mu d\mu.$$

Hence, by choosing  $\epsilon = 1/2$ ,

$$a_h(v_h, v_h) \geq \frac{1}{2} a_h^e(v_h, v_h) + \sum_{F \in \mathcal{F}_h^{v_i}} \frac{\alpha_F - C_{dt}}{H_F} \int_F \llbracket v_h \rrbracket^2 \mu d\mu,$$

from which we obtain the assertion.  $\square$

Discrete stability implies that the scheme (12) is well-posed, cf. [11, Lemma 1.30].

**Theorem 1** (Discrete well-posedness). Let  $\alpha_F \geq 1/2 + C_{dt}(k)$  with constant  $C_{dt}(k)$  given in Lemma 2. Then for any  $f \in L^2(\Omega)$  and  $g \in L^2(\Gamma; \mu)$  there exists a unique solution  $u_h \in V_h$  of the discrete variational problem (12).

*Proof.* The space  $V_h$  is finite-dimensional. Hence, Lemma 4 implies the assertion.  $\square$

To proceed with an abstract error estimate, we need the following boundedness result.

**Lemma 5** (Boundedness). For any  $u \in V_{*h}$  and  $v \in V_h$  it holds that

$$a_h(u, v) \leq (C_{dt} + \alpha_F) \|u\|_* \|v\|_{V_h},$$

where  $\alpha_F$  is as in Lemma 4.

*Proof.* We have that

$$\begin{aligned} a_h(u, v) &= a_h^e(u, v) - \sum_{F \in \mathcal{F}_h^{vi}} \int_F \left\{ \left\{ \frac{\mu}{\sigma_t} \partial_z^h u \right\} \right\} \llbracket v \rrbracket \mu d\mu - \sum_{F \in \mathcal{F}_h^{vi}} \int_F \left\{ \left\{ \frac{\mu}{\sigma_t} \partial_z^h v \right\} \right\} \llbracket u \rrbracket \mu d\mu \\ &\quad + \sum_{F \in \mathcal{F}_h^{vi}} \frac{\alpha_F}{H_F} \int_F \llbracket u \rrbracket \llbracket v \rrbracket \mu d\mu. \end{aligned}$$

The first two terms can be estimated using the Cauchy-Schwarz inequality as

$$\begin{aligned} a_h^e(u, v) &\leq a_h^e(u, u)^{1/2} a_h^e(v, v)^{1/2}, \\ \sum_{F \in \mathcal{F}_h^{vi}} \int_F \left\{ \left\{ \frac{\mu}{\sigma_t} \partial_z^h u \right\} \right\} \llbracket v \rrbracket \mu d\mu &\leq \sum_{F \in \mathcal{F}_h^{vi}} \left\| \left\{ \left\{ \frac{\mu}{\sigma_t} \partial_z^h u \right\} \right\} \right\|_{L^2(F; \mu)} \|\llbracket v \rrbracket\|_{L^2(F; \mu)}. \end{aligned}$$

For the third term, we use Lemma 3 to obtain

$$\sum_{F \in \mathcal{F}_h^{vi}} \int_F \left\{ \left\{ \frac{\mu}{\sigma_t} \partial_z^h v \right\} \right\} \llbracket u \rrbracket \mu d\mu \leq \sum_{F \in \mathcal{F}_h^{vi}} \frac{\sqrt{C_{dt}}}{2\sqrt{H_F}} \left( \left\| \frac{\mu}{\sigma_t} \partial_z v \right\|_{L^2(E_F^1)}^2 + \left\| \frac{\mu}{\sigma_t} \partial_z v \right\|_{L^2(E_F^2)}^2 \right)^{1/2} \|\llbracket u \rrbracket\|_{L^2(F; \mu)}.$$

To separate the terms that include  $u$  and  $v$ , respectively, we apply the Cauchy-Schwarz inequality once more and use again that each sub-element  $E_F^i$  touches at most two interior faces, to arrive at

$$\begin{aligned} a_h(u, v) &\leq \left( a_h^e(u, u) + \sum_{F \in \mathcal{F}_h^{vi}} \frac{H_F}{C_{dt}} \left\| \left\{ \left\{ \frac{\mu}{\sigma_t} \partial_z^h u \right\} \right\} \right\|_{L^2(F; \mu)}^2 + \frac{C_{dt} + \alpha_F}{H_F} \|\llbracket u \rrbracket\|_{L^2(F; \mu)}^2 \right)^{1/2} \\ &\quad \left( a_h^e(v, v) + \frac{1}{2} \left\| \frac{\mu}{\sigma_t} \partial_z^h v \right\|_{L^2(\Omega)}^2 + \sum_{F \in \mathcal{F}_h^{vi}} \frac{C_{dt} + \alpha_F}{H_F} \|\llbracket v \rrbracket\|_{L^2(F; \mu)}^2 \right)^{1/2}, \end{aligned}$$

which concludes the proof as  $C_{dt} + \alpha_F \geq 3/2$ .  $\square$

Before continuing, an inspection of the previous proof shows that we have the following corollary stating boundedness of  $a_h$  on  $V_h$ .

**Corollary 1** (Discrete boundedness). For any  $u, v \in V_h$  it holds that

$$a_h(u, v) \leq (C_{dt} + \alpha_F) \|u\|_{V_h} \|v\|_{V_h},$$

where  $\alpha_F$  is as in Lemma 4.

Combining consistency, stability and boundedness ensures that the discrete solution  $u_h$  to (12) yields a quasi-best approximation to  $u$ , cf. [11, Theorem 1.35].

**Theorem 2** (Error estimate). Let  $f \in L^2(\Omega)$  and  $g \in L^2(\Gamma; \mu)$ , and denote  $u \in V_*$  the solution to (1)–(2) and  $u_h \in V_h$  the solution to (12). Then the following error estimate holds true

$$\|u - u_h\|_{V_h} \leq (1 + 2(C_{dt}(k) + \alpha_F)) \inf_{v_h \in V_h} \|u - v_h\|_*,$$

provided that  $\alpha_F \geq 1/2 + C_{dt}(k)$ .

## 4 Numerical examples

In the following we confirm the theoretical statements about stability and convergence of Section 3 numerically. Let  $\sigma_s = 1/2$  and  $\sigma_t = 1$  and the width of the slab be  $L = 1$ . We then define the source terms  $f$  and  $g$  in (1)–(2) such that the exact solution is given by the following function

$$u(z, \mu) = (1 + \exp(-\mu)) \chi_{\{\mu > 1/2\}}(\mu) \exp(-z^2). \quad (14)$$

Here,  $\chi_{\{\mu > 1/2\}}(\mu)$  denotes the indicator function of the interval  $(1/2, 1)$ , i.e.,  $u$  is discontinuous in  $\mu = 1/2$ , but note that  $u \in V_*$ . We compute the DG solution  $u_h$  of (12) on a sequence of uniformly refined meshes, initially consisting of 16 elements, see Figure 1. Hence, the discontinuity in  $u$  is resolved by the mesh.

For our computations we use the spaces  $V_h$  with  $k = 0, 1, \dots, 4$  in eq. (7), that is piecewise polynomials of degree  $k$  in  $\mu$  and piecewise polynomials of degree  $k + 1$  in  $z$ . The value of  $C_{ie}$  of the inverse inequality in eq. (9) is computed by solving a small eigenvalue problem of dimension  $k + 1$ , which are obtained by transforming eq. (9) to the unit interval.

For the numerical solution of the resulting linear systems, we employ the usual source iteration [1]: Introducing the auxiliary bilinear form  $b_h(u, v) = a_h(u, v) - (\sigma_s P u, v)$ , the source iteration performs the iteration  $u_h^n \mapsto u_h^{n+1}$  by solving

$$b_h(u_h^{n+1}, v) = (\sigma_s P u_h^n, v) + (f, v) + \langle g, v \rangle \quad \forall v \in V_h. \quad (15)$$

The source iteration converges linearly with a rate  $\sigma_s/\sigma_t$  [1], which is bounded by  $1/2$  in this example. For acceleration of the source iteration by preconditioning see also [1, 31]. The matrix representation of  $b_h$  has a block structure for the uniformly refined meshes considered in this example, and its inverse can be applied efficiently via LU factorization.

Table 1 shows the broken and weighted  $H^1$ -norm of the error  $u - u_h$  between the exact and the numerical solution, defined as

$$\|v\|_{\mathcal{T}}^2 := \sum_{K \in \mathcal{T}} \left( \|\mu \partial_z^h v\|_{L^2(K)}^2 + \|v\|_{L^2(K)}^2 \right) \quad \forall v \in V_{*h}. \quad (16)$$

As expected from Theorem 2, we observe a convergence rate of order  $k + 1$  for the error.

**Tab. 1:** Error  $\|u - u_h\|_{\mathcal{T}}$  for different local polynomial degrees  $k$ , see eq. (7), and uniformly refined meshes with  $N$  elements and solution  $u$  defined in eq. (14).

$N$	16	64	256	1 024	4 096	16 384	65 536
$k = 0$	7.06e-02	3.53e-02	1.76e-02	8.81e-03	4.40e-03	2.20e-03	1.10e-03
$k = 1$	5.51e-03	1.38e-03	3.44e-04	8.60e-05	2.15e-05	5.37e-06	1.34e-06
$k = 2$	2.77e-04	3.47e-05	4.33e-06	5.41e-07	6.77e-08	8.46e-09	1.06e-09
$k = 3$	1.38e-05	8.69e-07	5.44e-08	3.40e-09	2.16e-10	4.18e-11	4.34e-11

## 5 Adaptivity

In this section we show, by examples, that hierarchical error estimators, see, e.g., [23] for the elliptic case, as well as estimators based on averaging the approximate solutions are a possible choice to adaptively construct optimal partitions  $\mathcal{T}$  of  $\Omega$  to approximate non-smooth solutions to eq. (1). In particular, we show how adaptive mesh refinement is beneficial if the discontinuity of the solution is not resolved by the mesh. To highlight the dependency on the partition  $\mathcal{T}$  of  $\Omega$  and on the polynomial degree, we will write  $u_{\mathcal{T},k}$  instead of  $u_h$  for the solution of the discontinuous Galerkin scheme (12). Similarly, we write  $V_{\mathcal{T},k}$  for the corresponding approximation space instead of  $V_h$ , see eq. (7). Let  $\mathcal{T}'$  be another partition of  $\Omega$  such that  $\mathcal{T} \subset \mathcal{T}'$ , and let  $k' \geq k$ . Denoting  $\|\cdot\|$  some norm defined on  $V + V_{\mathcal{T},k} + V_{\mathcal{T}',k'}$ , and supposing the saturation assumption, which has been used, e.g., also in [5],

$$\|u - u_{\mathcal{T}',k'}\| \leq \gamma \|u - u_{\mathcal{T},k}\|,$$

for some universal constant  $\gamma < 1$ , we obtain the equivalence between the approximation error and the estimator  $\zeta = u_{\mathcal{T}',k'} - u_{\mathcal{T},k}$ , i.e.,

$$(1 + \gamma)^{-1} \|\zeta\| \leq \|u - u_{\mathcal{T},k}\| \leq (1 - \gamma)^{-1} \|\zeta\|.$$

In the following numerical experiments, we use the norm  $\|\cdot\|_{\mathcal{T}}$  defined in (16) to investigate the behaviour of two hierarchical error indicators for different test cases. The local error contributions are then given by

$$\eta_K = (\|\mu\partial_z^h \zeta\|_{L^2(K)}^2 + \|\zeta\|_{L^2(K)}^2)^{1/2},$$

where  $K \in \mathcal{T}$ . The mesh is then refined by a Dörfler marking strategy [12, 34], that is all elements in the set  $\mathcal{K} \subset \mathcal{T}$  are refined, where  $\mathcal{K} \subset \mathcal{T}$  is the set of smallest cardinality such that

$$\sum_{K \in \mathcal{K}} \eta_K^2 > \theta \sum_{K \in \mathcal{T}} \eta_K^2, \quad (17)$$

where  $0 < \theta \leq 1$  is the bulk-chasing parameter. Differently from the previous section, we assume  $\sigma_t = 1$  and  $\sigma_s = 0$ . Moreover, we consider two different manufactured solution  $u_1$  and  $u_2$  given by

$$u_1(z, \mu) = (\mu^2 + z^2)^{1/4}, \quad (18)$$

$$u_2(z, \mu) = \left(1 + \chi_{\{\mu > 1/\sqrt{2}\}}(\mu)\right) \exp(-z^2). \quad (19)$$

The choice of  $1/\sqrt{2}$  in the indicator function ensures that the corresponding line discontinuity of  $u_2$  is never resolved by our mesh. Furthermore,  $\mu\partial_z u_1$  is bounded and vanishes in  $(0, 0)$ . In particular, we note that  $u_1, u_2 \in V_*$ . Eventually, the Dörfler parameter is set to  $\theta = 0.75$  in the following examples.

## 5.1 Hierarchical $p$ -error estimator

Setting  $\mathcal{T}' = \mathcal{T}$  and  $k' = k + 1$ , the hierarchical  $p$ -error estimator is defined as

$$\zeta_p = u_{\mathcal{T},k} - u_{\mathcal{T},k+1}. \quad (20)$$

We note that we used  $\alpha_F = 1/2 + C_{dt}(k+1)$  as a stabilization parameter for obtain both numerical solutions  $u_{\mathcal{T},k}$  and  $u_{\mathcal{T},k+1}$ .

Figure 2 and Figure 3 show the convergence rates for adaptively refined meshes using the  $\zeta_p$  indicator, for different values of the polynomial degree  $k$ . We observe that for the manufactured solution  $u_1$ , which has a point singularity in the origin, the indicator follows tightly the curve of the actual error. Moreover, the error decays as the optimal rate  $1/\sqrt{N^{k+1}}$ , with  $N$  denoting the number of degrees of freedom in  $V_{\mathcal{T},k}$ , also shown for comparison.

For the manufactured solution  $u_2$  with line discontinuity defined in eq. (19), the convergence rate is sub-optimal for  $k \geq 1$ , and also the error estimator is not as close to the true error anymore, compared to the test case with  $u_1$ . For  $k = 0$ , the error and the error estimator stay close, and follow the curve for the optimal rate.

## 5.2 Hierarchical $h$ -error estimator

Using once again the test cases eq. (19) and eq. (18), we now keep  $k' = k$  fixed and we construct  $\mathcal{T}'$  by uniform refinement of  $\mathcal{T}$ , i.e., every element in  $\mathcal{T}$  is subdivided in 4 new elements with halved edge length. The error estimator is now

$$\zeta_h = u_{\mathcal{T}',k} - u_{\mathcal{T},k}. \quad (21)$$

Some comments are due for the computation of  $u_{\mathcal{T}',k}$ , for which we use, as in definition (10) but with  $\mathcal{T}$  replaced by  $\mathcal{T}'$ , the bilinear form  $a_{h'} : V_{\mathcal{T}',k} \times V_{\mathcal{T}',k} \rightarrow \mathbb{R}$ . Since  $V_{\mathcal{T},k}$  is a subspace of  $V_{\mathcal{T}',k}$ , we require, similar to [23], that  $a_h$  is the restriction of  $a_{h'}$  to  $V_{\mathcal{T},k}$ , in the sense that

$$a_h(v, w) = a_{h'}(v, w) \quad \forall u, v \in V_{\mathcal{T},k}. \quad (22)$$

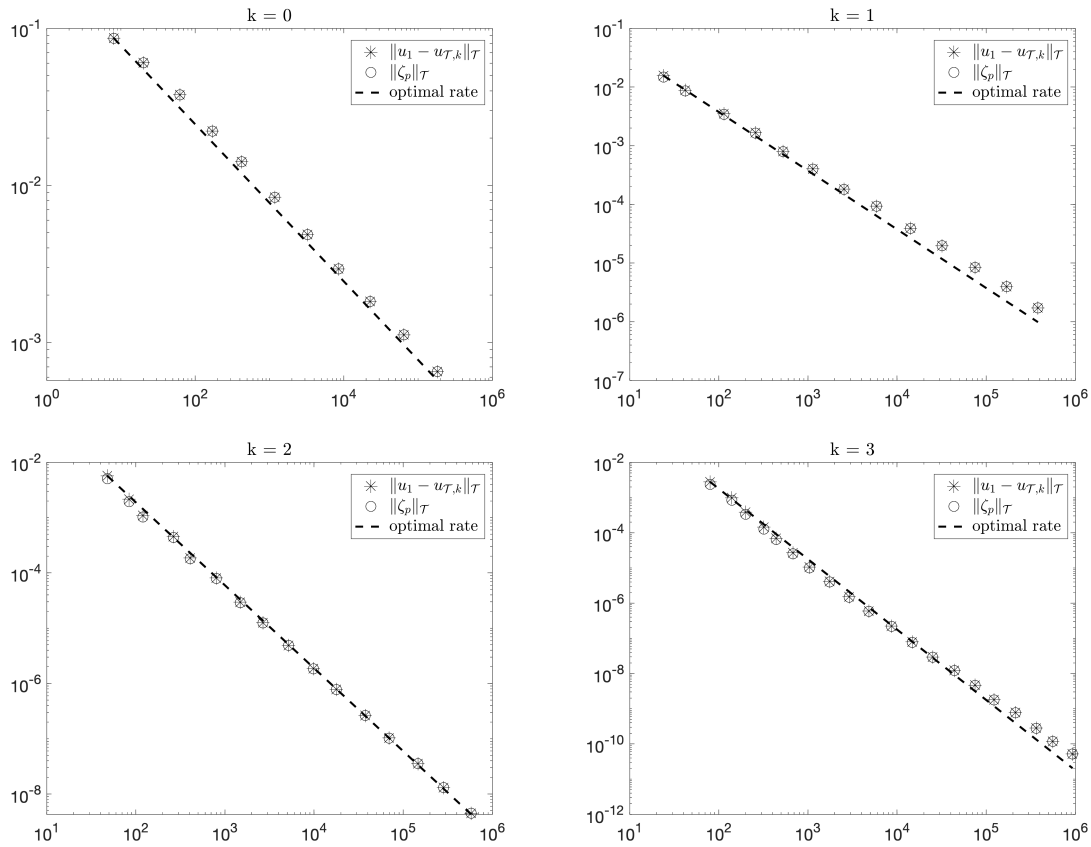


**Fig. 2:** Test case eq. (18) with singularity in  $(0,0)$ . Broken  $H^1$  norm of the approximation error and of the  $p$ -estimator plotted against the theoretical optimal rate, for different values of the starting polynomial degree  $k = 0, 1, 2, 3$ , in a double logarithmic scale.

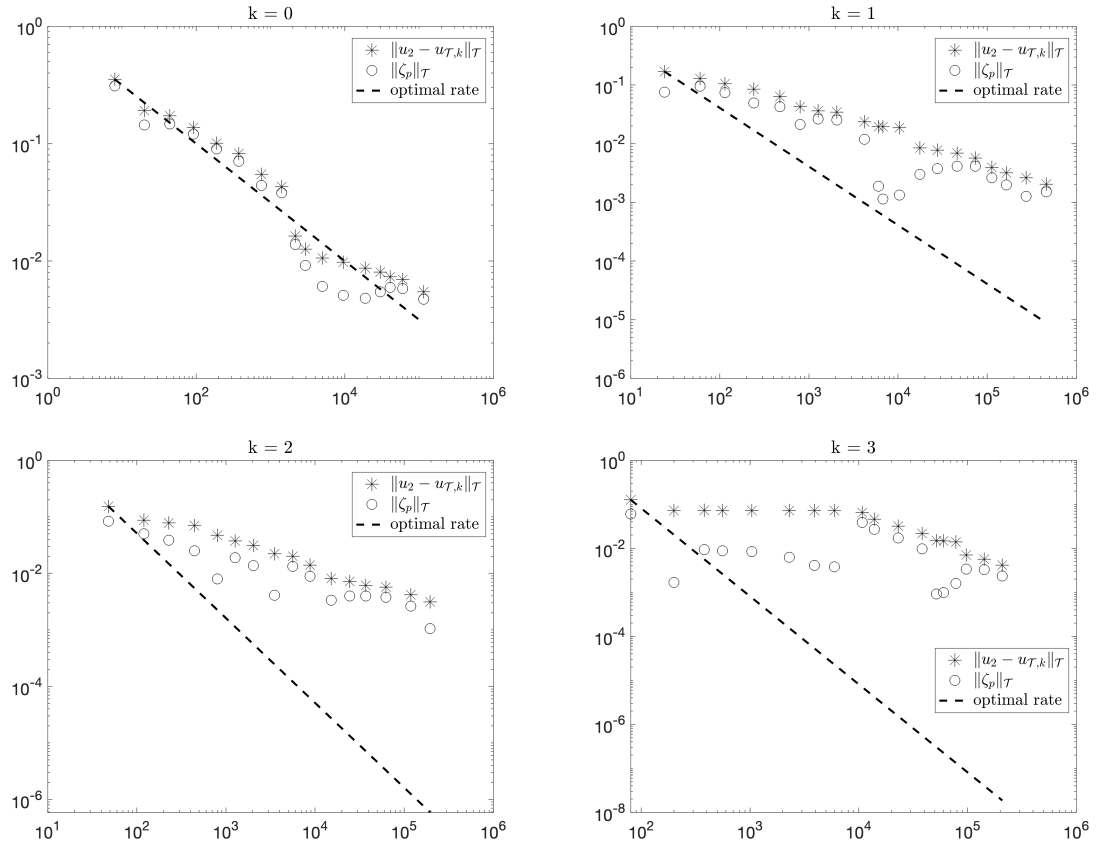


**Fig. 3:** Test case eq. (19) with discontinuity along the line  $\mu = 1/\sqrt{2}$ . Broken  $H^1$  norm of the approximation error and of the  $p$ -estimator plotted against the theoretical optimal rate, for different values of the starting polynomial degree  $k = 0, 1, 2, 3$ , in a double logarithmic scale.

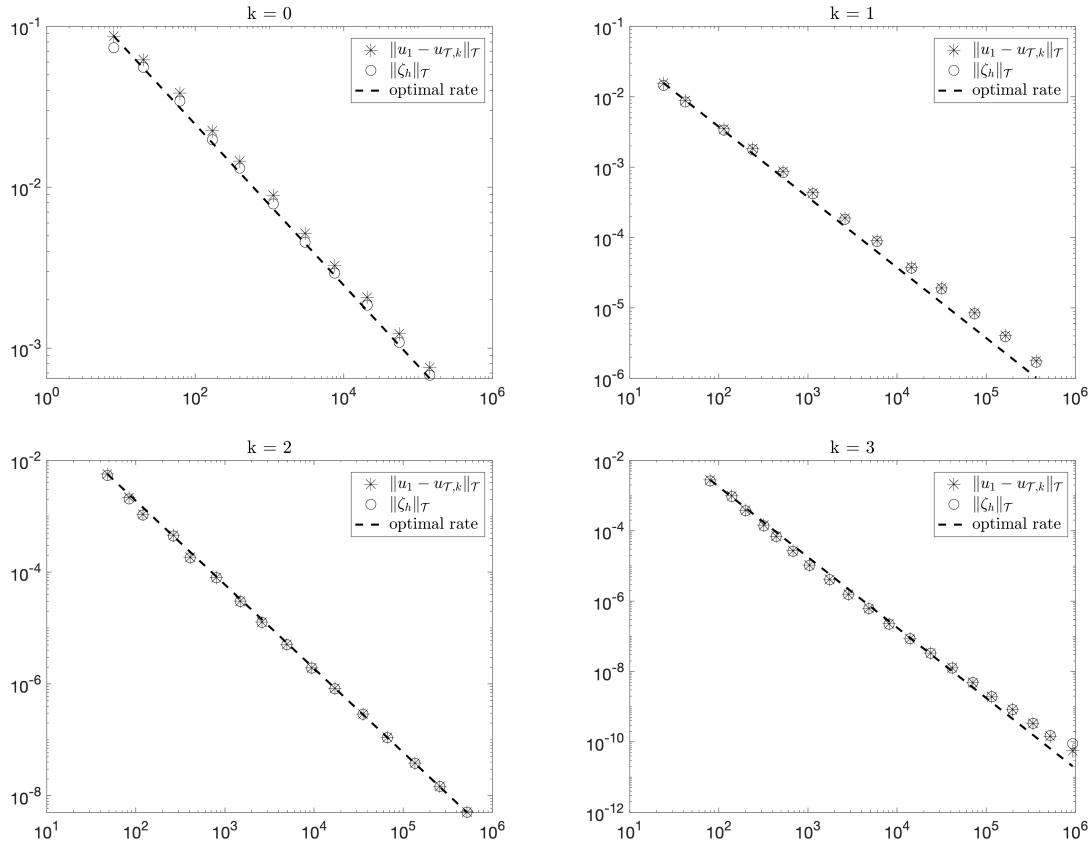


**Fig. 4:** Test case eq. (18) with singularity in  $(0, 0)$ . Broken  $H^1$  norm of the approximation error and of the  $h$ -estimator plotted against the theoretical optimal rate, for different values of the starting polynomial degree  $k = 0, 1, 2, 3$ , in a double logarithmic scale.

Comparing the penalty terms in  $a_h$  and  $a_{h'}$  shows that the above restriction is fulfilled if  $\alpha_F = 2\alpha'_F$ . Since we need to ensure discrete stability of both bilinear forms, we choose  $\alpha'_F = 1/2 + C_{dt}(k)$ .

Figure 4 and Figure 5 show the optimality of the estimator for the manufacture solution  $u_1$  with point singularity defined in eq. (18), and sub-optimality in the case of discontinuous exact solutions eq. (19), except for  $k = 0$ , where a similar comment as for the  $p$ -hierarchical estimator applies. We note that in all cases, the estimator is close to the actual error. Moreover, as shown in Figure 6 we observe that the estimator is able to detect the line discontinuity present in  $u_2$ . Moreover, the condition in eq. (22) is not essential for the results shown in this section. In fact, similar results can be obtained by using  $\alpha_F = \alpha_{F'} = 1/2 + C_{dt}(k)$ . The condition eq. (22) is required in the next section.

### 5.3 Error estimator based on the solution of local problems

Since the computation of the global error estimators  $\zeta$  presented in Section 5.1 and Section 5.2 is in general expensive, we investigate also an error estimator based on the solution of local problems, as presented in [16, 23] for corresponding elliptic problems. In this approach, the computed solution  $u_{T,k}$  is understood as the coarse-mesh approximation to some function, here  $u_{T',k}$ . Instead of using  $\zeta = u_{T,k} - u_{T',k}$  as before, local approximations  $\eta_K$  are computed element-wise.

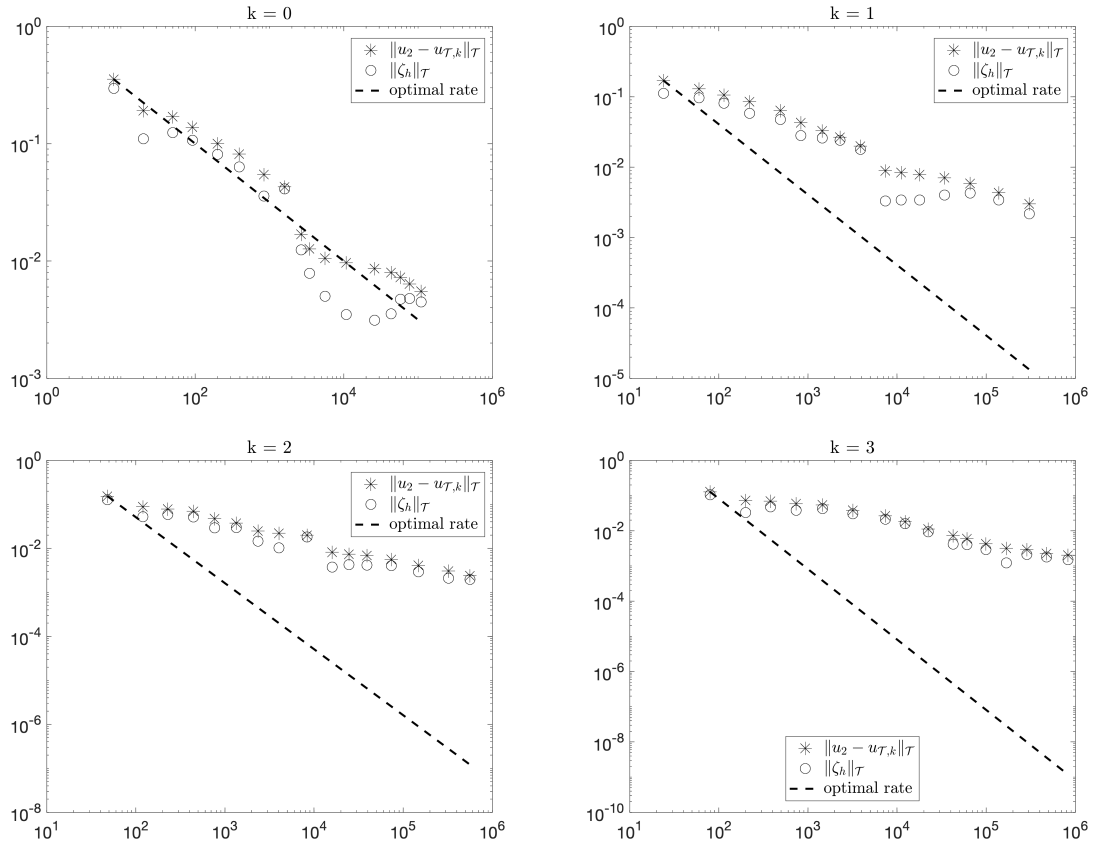


**Fig. 5:** Test case eq. (19) with line discontinuity. Broken  $H^1$  norm of the approximation error and of the  $h$ -estimator plotted against the theoretical optimal rate, for different values of the starting polynomial degree  $k = 0, 1, 2, 3$ , in a double logarithmic scale.

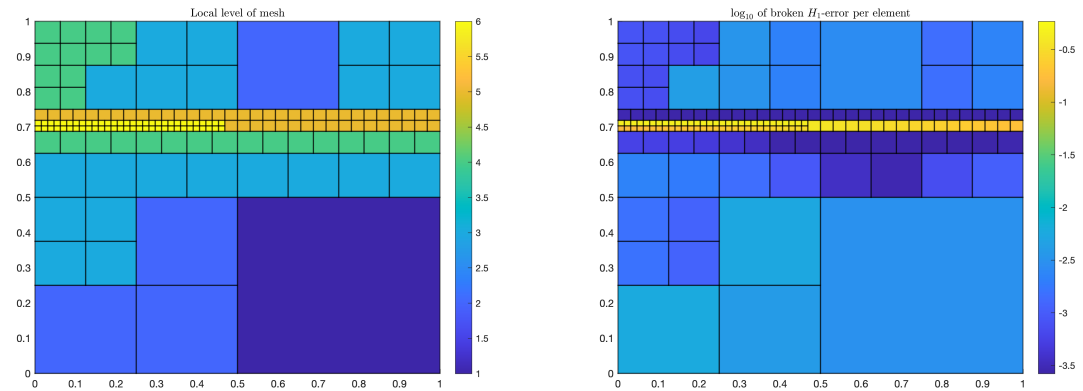


**Fig. 6:** Non-smooth test case eq. (19). Left: Locally refined mesh with local mesh sizes varying from  $1/2$  to  $1/2^6$  for  $N = 242$  elements. Top right: Local broken  $H^1$  approximation error for the grid shown left.

For each  $K \in \mathcal{T}$ , we consider the local space  $V_{\mathcal{T}',k}(K)$  obtained by restricting functions in  $V_{\mathcal{T}',k}$  to  $K$ . By extending functions in  $V_{\mathcal{T}',k}(K)$  to zero outside of  $K$ ,  $V_{\mathcal{T}',k}(K)$  becomes a subspace of  $V_{\mathcal{T}',k}$ . Indeed,

$$V_{\mathcal{T}',k} = \bigoplus_{K \in \mathcal{T}} V_{\mathcal{T}',k}(K). \quad (23)$$

On  $V_{\mathcal{T}',k}(K) \times V_{\mathcal{T}',k}(K)$  we introduce the (local) bilinear form  $a_{h'}^K$  as the restriction of  $a_{h'}$  to  $V_{\mathcal{T}',k}(K) \times V_{\mathcal{T}',k}(K)$ . This bilinear form inherits continuity and coercivity from  $a_{h'}$ . Using Lemma 4 there holds

$$a_{h'}^K(v, v) \geq \frac{1}{2} \|v\|_{V_{\mathcal{T}',k},K}^2, \quad (24)$$

where  $\|\cdot\|_{V_{\mathcal{T}',k},K}$  is the restriction of  $\|\cdot\|_{V_{\mathcal{T}',k}}$  to  $V_{\mathcal{T}',k}(K)$ . Here,  $\|\cdot\|_{V_{\mathcal{T}',k}}$  is defined according to eq. (13a) as

$$\|v\|_{V_{\mathcal{T}',k}}^2 = \|v\|_{\tilde{V}_{\mathcal{T}',k}}^2 + \sum_{F \in \mathcal{F}_{h'}^i} \frac{H'_F}{C_{dt}(k')} \left\| \left\{ \frac{\mu}{\sigma_t} \partial_z^h v \right\} \right\|_{L^2(F;\mu)}^2, \quad \forall v \in V_{\mathcal{T}',k}. \quad (25)$$

Let  $u_{\mathcal{T}',k'}$  be the discontinuous Galerkin approximation of  $u$  on  $V_{\mathcal{T}',k}$ , i.e.

$$a_{h'}(u_{\mathcal{T}',k'}, v) = (f, v) + \langle g, v \rangle \quad \forall v \in V_{\mathcal{T}',k}. \quad (26)$$

At this point we observe that (12), (22) and (26) imply  $\forall v \in V_h$ ,

$$\begin{aligned} a_{h'}(u_{\mathcal{T}',k'} - u_{\mathcal{T},k}, v) &= a_{h'}(u_{\mathcal{T}',k'}, v) - a_{h'}(u_{\mathcal{T},k}, v) \\ &= a_{h'}(u_{\mathcal{T}',k'}, v) - a_h(u_{\mathcal{T},k}, v) \\ &= (f, v) + \langle g, v \rangle - (f, v) - \langle g, v \rangle = 0. \end{aligned} \quad (27)$$

Eventually we introduce the functions  $\{\eta_K \in V_{\mathcal{T}',k}(K) | K \in \mathcal{T}_h\}$  as solutions to the local problems

$$a_{h'}^K(\eta_K, v) = a_{h'}(u_{\mathcal{T}',k} - u_{\mathcal{T},k}, v) = (f, v) + \langle g, v \rangle - a_{h'}(u_{\mathcal{T},k}, v) \quad \forall v \in V_{\mathcal{T}',k}(K). \quad (28)$$

Each  $\eta_K$  can be computed independently of each other and in parallel. The function  $\eta = \sum_{K \in \mathcal{T}} \eta_K \in V_{\mathcal{T}',k}$  then may serve as an approximation to the estimator  $\zeta = u_{\mathcal{T}',k} - u_h$  on  $V_{\mathcal{T}',k}$ , as in [23] for elliptic problems. Following [23, Theorem 4.1], we can prove a lower bound for  $\zeta$  in terms of the local error estimator  $\eta$ , i.e.

**Lemma 6.** We have that

$$\|\eta\|_{V_{\mathcal{T}',k}} \leq 2(C_{dt}(k) + \alpha'_F) \|\zeta\|_{V_{\mathcal{T}',k}}. \quad (29)$$

*Proof.* First of all we observe that the combination of (26) and (28) entails

$$a_{h'}^K(\eta_K, v) = a_{h'}(\zeta, v) \quad \forall v \in V_{\mathcal{T}',k}(K). \quad (30)$$

Plugging  $v = \eta_K \in V_{\mathcal{T}',k}(K)$  into the previous equation and recalling that  $\eta = \sum_K \eta_K$ , we have

$$\sum_{K \in \mathcal{T}} a_{h'}^K(\eta_K, \eta_K) = a_{h'}(\zeta, \eta) \leq (C_{dt}(k') + \alpha'_F) \|\zeta\|_{V_{\mathcal{T}',k}} \|\eta\|_{V_{\mathcal{T}',k}}, \quad (31)$$

where we used Corollary 1 in the last step. Coercivity of  $a_{h'}^K$ , expressed in (24), and eq. (23) entail

$$\sum_{K \in \mathcal{T}} a_{h'}^K(\eta_K, \eta_K) \geq \frac{1}{2} \sum_{K \in \mathcal{T}} \|\eta_K\|_{V_{\mathcal{T}',k},K}^2 \geq \frac{1}{2} \|\eta\|_{V_{\mathcal{T}',k}}^2. \quad (32)$$

Combining (31) and (32) we have eventually

$$\frac{1}{2} \|\eta\|_{V_{\mathcal{T}',k}}^2 \leq \sum_{K \in \mathcal{T}} a_{h'}^K(\eta_K, \eta_K) \leq (C_{dt}(k') + \alpha'_F) \|\zeta\|_{V_{\mathcal{T}',k}} \|\eta\|_{V_{\mathcal{T}',k}}, \quad (33)$$

which concludes the proof.  $\square$

Due to the lack of appropriate interpolation operators for functions in the space  $V$ , one cannot adapt the proofs given in [23] in a straight-forward fashion to show a bound of  $\zeta$  in terms of the local contributions  $\eta$ . In fact, some preliminary numerical tests, based on the broken  $H^1$ -norm eq. (16), suggest that the desired equivalence of  $\zeta$  and  $\eta$  might not be true. In a similar spirit, our preliminary numerical tests indicate that standard residual error estimators are either not reliable or efficient, which, again, may be explained by the lack of suitable interpolation error estimates required to obtain the correct scaling in terms of the local mesh size of the different local contributions, cf., [11, Section 5.6] or [3, 34]. Therefore, we investigate in the next section another error estimator based on local averages.

## 5.4 Error estimator based on averaging the approximate solution

In the context of a posteriori error estimation and adaptive mesh refinement, ZZ-error estimators named after Zienkiewicz and Zhu [35] are widely used in practice. Compared to the previously mentioned hierarchical error estimators, their major advantage is the fact that no further mesh nor a further solution is required. In order to obtain a reliable error estimator, one simply takes a discontinuous  $u_h \in V_h$  and approximates it by some continuous piecewise linear polynomial  $\tilde{u}_h$  by a post-processing step. In the presence of a geometrically conforming triangulation, such a continuous piecewise polynomials  $\tilde{u}_h$  can be described as a linear combination of the well-known Lagrange nodal basis functions. However, our approximation involves hanging nodes and we therefore restrict the construction to the set of regular nodes  $\mathcal{N}_h$ . For a node  $\nu \in \mathcal{N}_h$ , we define by  $\omega_\nu$  the union of all elements of  $K \in \mathcal{T}$  sharing the vertex  $\nu$ . Then, we construct the continuous piecewise linear averaging  $\tilde{u}_h$  such that

$$\tilde{u}_h(\nu) = \sum_{K \in \mathcal{T}, K \subset \omega_\nu} \frac{|K|}{|\omega_\nu|} u_h|_K(\nu) \quad (34)$$

holds for each regular node  $\nu \in \mathcal{N}_h$ . The averaging error estimator is then defined by

$$\eta_A^2 = \sum_{K \in \mathcal{T}} \|u_h - \tilde{u}_h\|_{L^2(K)}^2, \quad (35)$$

where the local contributions are used to refine the mesh using Dörfler marking as described above. Figure 7 shows the convergence rates for adaptively refined meshes using the averaging indicator for the test eq. (19). The indicator behaves correctly and replicates the curve of the actual error. These curves have the same slope as the optimal rate  $1/\sqrt{N}$  curve, with  $N$  number of elements in the quad-tree mesh, also shown for comparison. In comparison to the hierarchical estimators, cf. fig. 3 and fig. 5, the averaging error estimator follows the actual error curve more closely.

## 6 Conclusions

We developed and analyzed a discontinuous Galerkin approximation for the radiative transfer equation in slab geometry. The use of quad-tree grids allowed for a relatively simple analysis with similar arguments as for more standard elliptic problems. While such grids allow for local mesh refinement in phase-space, the implementation of the numerical scheme is straightforward. For sufficiently regular solutions, we showed optimal rates of convergence.

We showed by example that non-smooth solutions can be approximated well by adaptively refined grids. In order to automate the mesh adaptation procedure, an error estimator is required. We investigated numerically hierarchical error estimators and estimators based on local averaging in a post-processing step. All three estimators closely follow the actual error, and, in the case of line singularities, they can be used to obtain optimal convergence rates. We note that the hierarchical error estimators require to solve global problems, and it is left for future research to investigate whether a localization is possible. Upper bounds

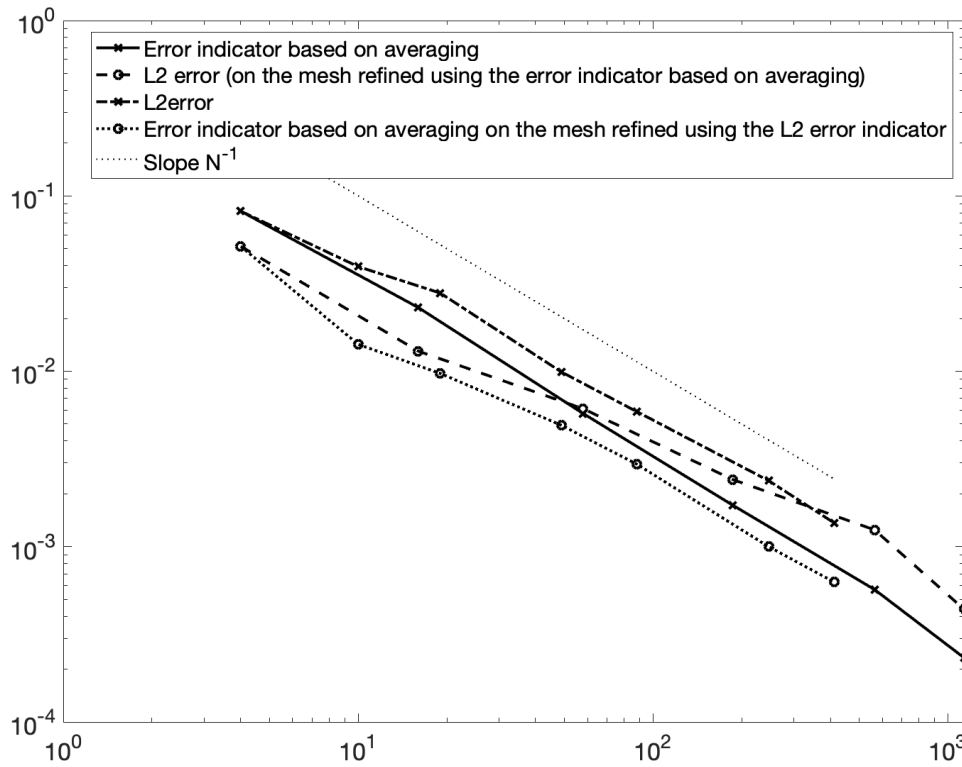
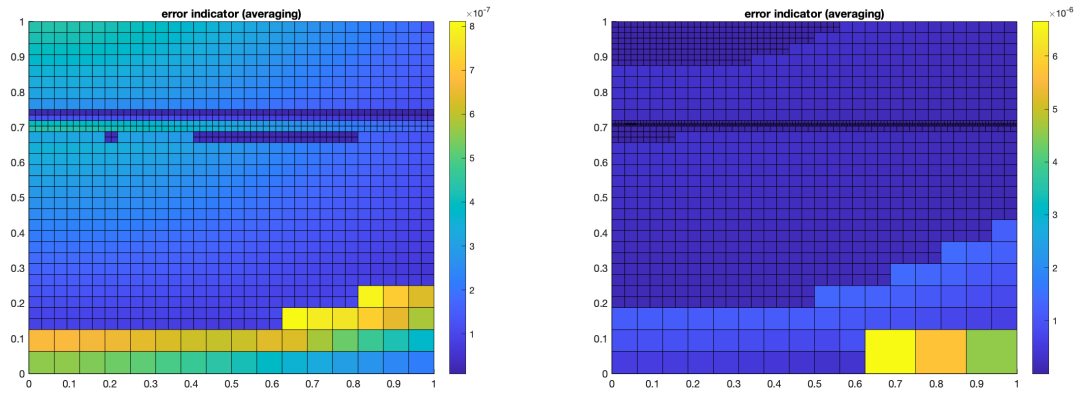


**Fig. 7:** Non-smooth test case eq. (19). Top left: Locally refined mesh with the average error estimator after 6 refinements. Top right: Locally refined mesh with the true  $L^2$  error used as an error indicator for comparison. Bottom: Convergence of the averaging error estimator, on adaptively refined grids using the averaging error estimator (solid line) and the exact error on this grid (dashed line with o), as well as the rate  $1/N$  (light dotted line) in a double logarithmic scale. For comparison, we show an error indicator using the true  $L^2$ -error (dash-dotted with x) and the corresponding averaging error estimator on that grid (dotted with o).

for the error can be derived for consistent approximations using duality theory [20]. Rigorous a posteriori error estimation has also been done using discontinuous Petrov-Galerkin discretizations [9]. We leave it to future research to analyze the error estimators for the discontinuous Galerkin scheme considered here.

While the solution of the linear systems for uniformly refined grids can be implemented using the established preconditioned iterative solvers [1, 31], the structure of the linear systems for adaptively refined grids is more complex because the equations do not fully decouple in  $\mu$ ; compare the situations in Figure 1. One possible direction is to develop nested solvers, or to adapt the methodology of [32]. We leave this for future research.

## Acknowledgements

RB and MS acknowledge support by the Dutch Research Council (NWO) via grant OCENW.KLEIN.183. <http://dx.doi.org/10.13039/501100003246>, "Nederlandse Organisatie voor Wetenschappelijk Onderzoek".

## References

- [1] M. L. Adams and E. W. Larsen. Fast iterative methods for discrete-ordinates particle transport calculations. *Progress in Nuclear Energy*, 40(1):3–159, 2002.
- [2] V. Agoshkov. *Boundary Value Problems for Transport Equations*. Modeling and Simulation in Science, Engineering and Technology. Birkhäuser, Boston, 1998.
- [3] Mark Ainsworth and J. Tinsley Oden. *A posteriori error estimation in finite element analysis*. Pure and Applied Mathematics (New York). Wiley-Interscience [John Wiley & Sons], New York, 2000.
- [4] D. Arnush. Underwater light-beam propagation in the small-angle-scattering approximation. *Journal of the Optical Society of America*, 62(9):1109, sep 1972.
- [5] Randolph E. Bank and R. Kent Smith. A posteriori error estimates based on hierarchical bases. *SIAM Journal on Numerical Analysis*, 30(4):921–935, 1993.
- [6] Susanne C. Brenner and L. Ridgway Scott. *The mathematical theory of finite element methods*. Springer, 3 edition, 2008.
- [7] T. Burger, J. Kuhn, R. Caps, and J. Fricke. Quantitative determination of the scattering and absorption coefficients from diffuse reflectance and transmittance measurements: Application to pharmaceutical powders. *Appl. Spectrosc.*, 51(3):309–317, Mar 1997.
- [8] Rémi Carminati and John C. Schotland. *Principles of Scattering and Transport of Light*. Cambridge University Press, jun 2021.
- [9] Wolfgang Dahmen, Felix Gruber, and Olga Mula. An adaptive nested source term iteration for radiative transfer equations. *Mathematics of Computation*, 89(324):1605–1646, 2020.
- [10] Valmor F De Almeida. An iterative phase-space explicit discontinuous Galerkin method for stellar radiative transfer in extended atmospheres. *Journal of Quantitative Spectroscopy and Radiative Transfer*, 196:254–269, 2017.
- [11] Daniele Antonio Di Pietro and Alexandre Ern. *Mathematical aspects of discontinuous Galerkin methods*, volume 69 of *Mathématiques & Applications (Berlin) [Mathematics & Applications]*. Springer, Heidelberg, 2012.
- [12] Willy Dörfler. A convergent adaptive algorithm for poisson's equation. *SIAM Journal on Numerical Analysis*, 33(3):1106–1124, jun 1996.
- [13] J. J. Duderstadt and W. R. Martin. *Transport Theory*. John Wiley & Sons, Inc., New York, 1979.
- [14] H. Egger and M. Schlottbom. A mixed variational framework for the radiative transfer equation. *Math. Mod. Meth. Appl. Sci.*, 22:1150014, 2012.
- [15] Y Favennec, T Mathew, MA Badri, Pierre Jolivet, Benoit Rousseau, D Lemonnier, and PJ Coelho. Ad

- hoc angular discretization of the radiative transfer equation. *Journal of Quantitative Spectroscopy and Radiative Transfer*, 225:301–318, 2019.
- [16] Xiaobing Feng and Ohannes A. Karakashian. Two-level additive schwarz methods for a discontinuous galerkin approximation of second order elliptic problems. *SIAM Journal on Numerical Analysis*, 39(4):1343–1365, 2002.
- [17] Pascal Jean Frey and Paul-Louis George. *Mesh Generation - Applications to Finite Elements*. John Wiley & Sons Inc., 2nd edition, 2008.
- [18] David Gilbarg and Neil S. Trudinger. *Elliptic partial differential equations of second order*. Classics in Mathematics. Springer-Verlag, Berlin, 2001. Reprint of the 1998 edition.
- [19] Jean-Luc Guermond, Guido Kanschat, and Jean C Ragusa. Discontinuous Galerkin for the radiative transport equation. In *Recent developments in discontinuous Galerkin finite element methods for partial differential equations*, pages 181–193. Springer, 2014.
- [20] Weimin Han. A posteriori error analysis in radiative transfer. *Applicable Analysis*, 94(12):2517–2534, dec 2014.
- [21] Weimin Han, Jianguo Huang, and Joseph A. Eichholz. Discrete-ordinate discontinuous galerkin methods for solving the radiative transfer equation. *SIAM Journal on Scientific Computing*, 32(2):477–497, 2010.
- [22] James E. Hansen and Larry D. Travis. Light scattering in planetary atmospheres. *Space Science Reviews*, 16(4):527–610, oct 1974.
- [23] Ohannes A. Karakashian and Frederic Pascal. A posteriori error estimates for a discontinuous galerkin approximation of second-order elliptic problems. *SIAM Journal on Numerical Analysis*, 41(6):2374–2399, jan 2003.
- [24] Gerhard Kitzler and Joachim Schöberl. A high order space–momentum discontinuous Galerkin method for the boltzmann equation. *Computers & Mathematics with Applications*, 70(7):1539–1554, 2015.
- [25] Daniel Kitzmann, Jan Bolte, and A Beate C Patzer. Discontinuous Galerkin finite element methods for radiative transfer in spherical symmetry. *Astronomy & Astrophysics*, 595:A90, 2016.
- [26] József Kópházi and Danny Lathouwers. A space–angle DGFEM approach for the Boltzmann radiation transport equation with local angular refinement. *Journal of Computational Physics*, 297:637–668, 2015.
- [27] LH Liu. Finite element solution of radiative transfer across a slab with variable spatial refractive index. *International journal of heat and mass transfer*, 48(11):2260–2265, 2005.
- [28] William R Martin and James J Duderstadt. Finite element solutions of the neutron transport equation with applications to strong heterogeneities. *Nuclear Science and Engineering*, 62(3):371–390, 1977.
- [29] William R Martin, Carl E Yehmert, Leonard Lorence, and James J Duderstadt. Phase-space finite element methods applied to the first-order form of the transport equation. *Annals of Nuclear Energy*, 8(11-12):633–646, 1981.
- [30] Rustamzhon Melikov, Daniel Aaron Press, Baskaran Ganesh Kumar, Sadra Sadeghi, and Sedat Nizamoglu. Unravelling radiative energy transfer in solid-state lighting. *Journal of Applied Physics*, 123(2):023103, jan 2018.
- [31] Olena Palii and Matthias Schlottbom. On a convergent DSA preconditioned source iteration for a DGFEM method for radiative transfer. *Computers and Mathematics with Applications*, 79(12):3366–3377, 2020.
- [32] Will Pazner and Tzanio Kolev. Uniform subspace correction preconditioners for discontinuous galerkin methods with hp-refinement. *Communications on Applied Mathematics and Computation*, 4(2):697–727, Jun 2022.
- [33] Jean C Ragusa and Yaqi Wang. A two-mesh adaptive mesh refinement technique for SN neutral-particle transport using a higher-order DGFEM. *Journal of computational and applied mathematics*, 233(12):3178–3188, 2010.
- [34] Rüdiger Verfürth. *A Posteriori Error Estimation Techniques for Finite Element Methods*. Oxford University Press, apr 2013.



- [35] O.C. Zienkiewicz and J.Z. Zhu. The superconvergent patch recovery and a posteriori error estimates. part 1: The recovery technique. *Int. J. Num. Meth. Engng.* 33, pages 1331–1364, 1992.